Numerical Validation of an Innovative Fish Baffle Design in Response to Fish Passage Issues at Perched Culverts

Jason Duguay[1]*, Jay Lacey[2]

Abstract
The hydraulic characteristics of a half-round corrugated steel fish ladder is investigated by means of an advanced numerical model. The objective of this study was to develop an innovative baffle design which produces an appropriate flow field for fish passage over a wide range of seasonal flow rates. The baffle consists of a lower main passageway, to accommodate fish passage at low flow rates, and a higher secondary passageway, which presents an auxiliary option for fish passage as well as debris at higher discharges. The elevated center arch of the baffle develops pool depth, thus minimizing the volumetric dissipative power in the pools at high flow rates. The velocities at the passageways respect critical swim speeds for a wide range of fish species of socioeconomic importance to North America. Turbulence metrics (turbulent kinetic energy and volumetric dissipative power) within the 3D dimensional flow structure of the pool are also investigated and discussed. The presence of a large hydraulic refuge zone was identified in the upstream section of the pools which fish may use to stage jumping attempts. The proposed fish ladder, made of polymer coated corrugated steel is a lightweight, durable and low cost solution to the problem of aquatic habitat fragmentation at perched culverts.

Keywords
Perched culverts, Fish passage, Fish ladders, Corrugated Steel, Fisheries management

[1] *Department de génie civil, University of Sherbrooke, Sherbrooke, Québec, Canada*
[2] *Department de génie civil, University of Sherbrooke, Sherbrooke, Québec, Canada*
***Corresponding author**: jason.duguay@usherbrooke.com

Contents

1. Introduction

Barriers to fish migration caused by perched culverts are an unfortunate reality of the extensive road and rail networks that span North America. Perched culverts are developed by a combination of scour and bed sediment transport phenomena and have been shown to have an important influence on the population distribution of fish species ([1],[2],[3],[4]). Through erosive processes an excessively large scour hole can develop at the downstream end of improperly designed culverts. The resulting vertical drop from the culvert invert to the water surface level of the outlet pool can vary anywhere between a few centimeters and 2 m or more. Mildly perched culverts are likely passable for fish species with stronger jumping capacities, yet culverts with large drops pose a significant fish passage barrier. Furthermore, perched culverts are often located beneath a significant depth of earth fill used to support road or rail infrastructure. Replacement of perched culverts with culverts designed to prevent perching is, in many cases, unrealistic given the high costs associated with removing the fill and the inevitable inconveniences to the public caused by blocking road lanes and or rail lines. In light of these realities, many perched culverts go unaddressed. Remedying these problems with conventional fish ladders or fishway designs is often a very labor and resource intensive solution since many perched culverts are found on difficult terrain, or in remote regions not conducive to conventional construction practices (e.g. concrete form work, heavy machinery). Given these considerations, a readily installed, light-weight and economical fish ladder would be beneficial in order to address fish passage

issues at the majority of perched culverts.

2. Background

2.1 Fish Passage Stressors

A report by the Departement of Fisheries and Oceans (Canada) presents a list of multiple stressors known to inhibit fish passage at in-stream anthropogenic structures [5]. Among these stressors, a few are of particular importance for the design of a fish ladder. The flow field of the Hannaford fishway will be evaluated for its response to the following four stressors; inadequate water depths, excessive velocities, substantial vertical drops and elevated turbulence levels. Numerous independent research efforts have investigated the effects of these four stressors on fish passage performance on indigenous North American species and the following subsections touch on the principle findings of these studies and highlight those of particular interest for evaluating the flow field of the fish ladder.

2.1.1 Barrier velocities

Fish have three swim speed modes. The fastest of the three is termed the *burst speed* (sometimes critical speed) and is used normally only to evade predators and navigate rapid reaches or sections of a river such as a choke or a low level cascade. A fish's burst-speed can only be maintained for a brief period (a couple of seconds) and recuperation is needed after its use. In contrast, a fish's *sustained speed* can be held for a duration of a couple of minutes. Fish use their sustained speed to traverse swift reaches of a river. Finally, the *cruising speed* is maintainable for an indefinite period of time and is used for feeding or migrating over slower reaches of water [6].

The velocity thresholds that distinguish these three swimming speeds depend, on among others, but primarily; the species of fish, body length, its maturity and ambient water temperature ([6], [7]). Burst-speed of target species is a critical design parameter to consider when selecting the geometry of the baffle. Excessive velocities in the pool can also diminish the availability of suitable zones of hydraulic refuge. Over the last half a century many studies have been performed with the intent of defining critical swimming speeds for a variety of fish species. A comprehensive study examined various authors' attempts at quantifying swimming speed thresholds for fishes of social and economic importance (Fig. 1) [8]. Brown trout (*Salmo trutta*) and Cutthroat trout (*Oncorhynchus clarkii*) figure among the species listed in Fig. 1) as well as their range of swim speeds. An another important species, the Artic char (*Salvelinus alpinus*) is not shown in Fig. 1), however this specie's range of critical swimming speeds is known to be between 41.1 to 97.2 cm/s [9]. The velocity ranges presented in Fig. 1 can be used to identify potential barriers at fish passage structures such as the fish ladder in the present study.

2.1.2 Turbulence

Turbulence is defined as the random fluctuations of velocity and vorticity around a statistically steady mean of these parameters. Many studies have investigated the influence of turbulence on fish passage, with the majority focusing on how turbulence affects preferred holding positions and swimming energetics. Fish have been found to prefer zones of low turbulence ([10], [11]). Excessive turbulence has been shown to significantly reduce fish passage success rates in a pool and weir fishway [12]. Many metrics exist which can be used to characterize the level of turbulence in a flow (e.g. TKE, VDP, turbulent intensity, Reynold's shear stress). A number of studies have used the volumetric dissipated power (VDP) to measure the bulk turbulence within pool type fishways ([13], [14], [12]). VDP, with units of W/m^3, gives a global evaluation of the turbulence within a region of flow. Recommended values vary between 150 W/m^3 and 200 W/m^3, depending on the size and species of the target fish (150 W/m^3 for trout and 200 W/m^3 for salmon) [15]. Equation 1 is used to calculate VDP (Pv) with ρ as density (kg/m^3), Q flow rate (m^3/s) and Δh being the elevation drop between the pools of the fish ladder.

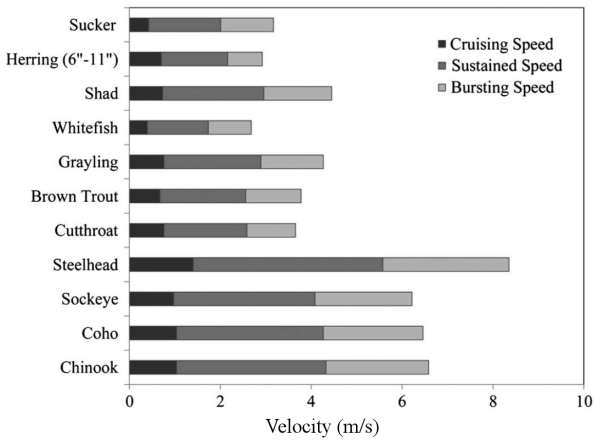

Figure 1. Adult fish swimming speeds (from Olsen and Tullis 2013 with reference to Bell 1990).

$$P_v = \rho g Q \frac{\Delta h}{V} \tag{1}$$

Turbulent kinetic energy (TKE), on the other hand, gives a more local evaluation of turbulence compared to the VDP and can be useful to identify zones of elevated turbulence, undesirable for fish locomotion and holding stations. TKE is defined as the sum of the variance of the three velocity components at a point in the flow where $i = u, v, j$ and $TKE = 0.5(\sigma_u^2 + \sigma_v^2 + \sigma_w^2)$, where σ_i is the standard deviation.

2.1.3 Jump height, pool depth and passageway width

Various researches have investigated the jumping capacities of trout and salmon species ([16], [17], [18], [19], [20]). These research efforts have demonstrated that passage success depends not only on the height of the vertical drop but also on the depth of the pool and the width of the passageway. Adequate pool depth is necessary to ensure that fish can accelerate to velocities needed to propel themselves over the

obstacle. Brandt et al. (2005) suggest that fish passes designed for juvenile brook trout (*Salvelinus fontinalis*) should have a maximum drop height of 0.1 m, pool depth of 0.1 m (but, should be as deep as possible) and a slot width as wide as possible. Another study demonstrated that brook trout with body lengths between 0.10-0.15 m could jump a staggering 0.64 m and larger size fish could reach heights of 0 [19]. 74 m. The DFO provides values of Δh of varying from 100 mm for streams on small watersheds (<2.5km^2) up to 200 mm for larger watersheds for use in baffle designs in road culvert design [5].

2.1.4 Hydraulic and Predatory refuge

Hydraulic refuge can be characterized by zones of low average velocity and turbulence levels compared to the mean values present in the surrounding flow. These regions should also be free of surging upwells, downwells and high levels of turbulent agitation. Ascending fish take advantage of these relatively tranquil regions in the flow to rest and then stage burst efforts through the next upstream passageway. Failure to ensure that adequate hydraulic refuge is available over the length of the fish ladder will compromise its effectiveness.

3. The Hannaford Baffle

The present study employs a 3D computational fluid dynamic model (CFD) to investigate the hydraulic characteristics of an innovative fish baffle form presented in Fig. 2. The Hannaford baffle, as it is referred to hereafter, was arrived at after numerous simulations of various design modifications. The presented baffle design is not necessarily final, rather an acceptable starting point from which field verification can be performed to provide insights on possible modifications for improvements. The Hannaford baffle consists of a lower principal passageway and a higher secondary passageway. The two passageways are separated by an arch which protrudes the water surface under all but the highest flow rates. In Fig. 2, θ and ϕ are the radii of the principal and secondary passageway, Y is the depth between the bottom of the baffle and the lowest point of the principal passageway, φ is the distance from the lowest point of the principal passageway and the highest point of the baffle, and finally y is the distance from the bottom of the baffle to the lowest point of the principal baffle. The front view of the downstream facing ramp is also shown in Fig. 2. The ramp which respects a 2:1 slope beginning at the lowest point in the trough of the principal passageway and extends outwards by a distance of 0.2 m.

The arch serves to direct flow through the principal and secondary passageways and also to retain water and increase the depth of the pool. The wide lower passageway is thought to provide fish with a large surface area for upstream passage. This design feature is in line with recommendations from a study by Brandt et al. (2005) on juvenile brook trout which showed that increasing width of vertical obstacles significantly improved jumping success rates. The curved form of the baffle is intended to reduce blockages by eliminating abrupt edges for debris to catch upon, thus minimizing maintenance requirements.

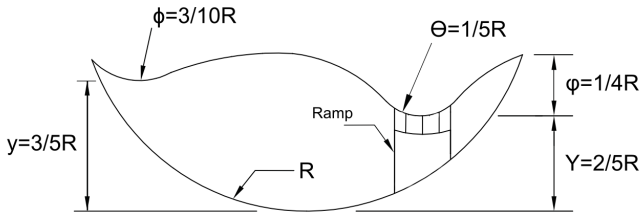

Figure 2. Approximate dimensions of the Hannaford baffle relative to the culvert radius, *R*.

The baffle spacing of the numerical model was chosen to respect these design considerations with a Δh of 200 mm. This is 10 cm higher than the maximum 10 cm Δh suggested for juvenile brook trout by Brandt et al. (2005). However the present study intends to be as general as possible by designing a fish ladder that can be used for commonly larger watersheds and therefore a Δh of 200 mm was retained.

The fish ladder design in the present numerical simulation will be evaluated for its presence of hydraulic refuge. This will be achieved by investigating the 3-dimensional flow field of the inter-baffle region for strong 3-dimensional flow phenomena (upwelling, downwelling and presence of vortices) as well as zones exhibiting velocities higher than the sustained swim speed range of the species listed in Fig. 1.

The principal passageways of the baffle are offset over the entire length of the fish ladder. A recent study found that in an orifice pool and weir type fishway, offsetting the orifices markedly improved the successful ascension rates compared to a straight orifice arrangement [21]. Velocities in the recirculation region of the pool were considerably reduced for the offset orifice arrangement. Despite the fact that Silva et al. (2012) investigated submerged orifices, it is likely that similar reductions in velocities will be achieved by offsetting the Hannaford baffle.

4. Numerical model

4.1 Introduction

An advanced computational fluid dynamics (CFD) software package (Flow-3D distributed by Flow Science Inc.) was employed to gain insights into the 3D flow field of the fish ladder. CFD offers the advantage of enabling the designer to test numerous geometries without the need to commit to resource intensive physical models. The results of the simulation are most useful for honing the design of a physical prototype for further development and field validation. The numerical code employed here solves the Reynolds averaged Navier-Stokes equations with a coupled two equation k-ε turbulence closure model. The k-ε model was applied for its ability to give reasonable approximations of free surface flows [22].

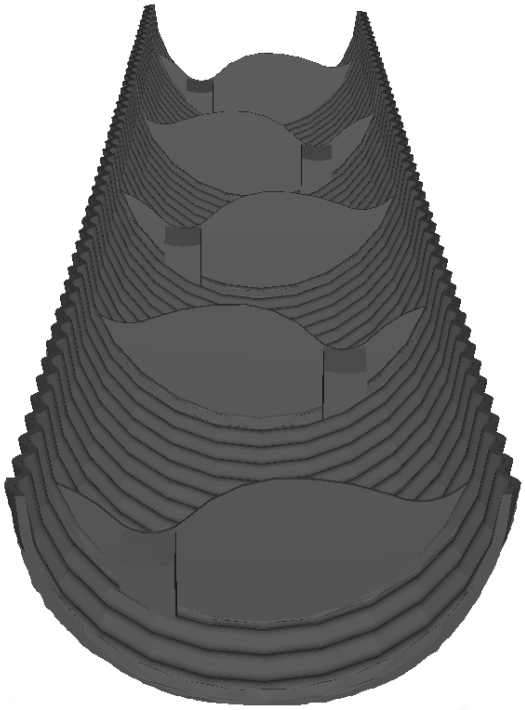

Figure 3. CAD representation of the numerically simulated fish ladder.

4.2 Model Configuration

A three dimensional computer assisted design (CFD) model of the fish ladder (see Fig. 3 was first drawn and then imported into Flow 3D as a stereolithography file. The fish ladder had the following characteristics; a length of 10 m, a diameter of 2.44 m and corrugations with a pitch of 0.230 mm, a depth of 0.064 mm and a radius of 0.057 mm. The fish ladder was set on a slope of 8.5%. The dimensions of the numerical fish ladder were chosen to fit those needed to install a physical prototype ladder on a actual perched culvert located in Newfoundland, Canada. This culvert is an ideal candidate for future in-situ testing. Stereolithography files accurately represent the surfaces of 3D objects as an array of interconnected triangular facets. Flow 3D has an integrated function which allows the program to accurately resolve complex geometrical surfaces represented by stereolithography files such as the corrugations in the current study. Baffles were separated by a distance of 2.37 m starting at 0.75 m from the upstream end of the fish ladder. Baffle spacing was chosen to respect the 200 mm Δh suggested by the DFO [5]. The principal passageway alternates position from left to right over the entire length of the fish ladder as can be seen in Fig. 3. The 0.200 m long ramp downstream of each principal passageway are also visible in Fig. 3.

4.2.1 Mesh Generation and Flux surfaces

The employed numerical code requires the user to generate structured mesh blocks to discretize the computational domain. A group of six mesh blocks with cell sizes of 25 mm were created to define the computational domain around the ladder. Domain removing components were applied to reduce the number of unnecessary cells with the objective of reducing simulation times. Visual verification of Flow-3D's representation of the baffle and corrugation geometries confirmed that a 25 mm cell size produced sufficient resolution. Given the minimum cell size, the thickness of the baffles was set at 25 mm instead of the thickness of polymer coated steel (6 mm) which would be used to fabricate the actual baffles. The use of a thicker baffle in the numerical model allows the geometries to be resolved without resorting to excessively small cell sizes which necessitate long simulation times (in the order of weeks). The additional thickness is believed to have only minor effects on the simulated flow field. Porous flux surfaces were defined at each of the baffles to record the flow rates passing over each baffle at a given period in time during the simulation. The flux surface data output was used in conjunction with the time dependent mass averaged mean kinetic energy to determine when the simulation was sufficiently close to a steady-state solution. Once the flow rates over each of the baffles were in close accordance and the mass averaged mean kinetic energy had stabilized over a sufficient period of time (4 to 8 seconds) the simulation was terminated.

4.2.2 Boundary and Initial Conditions

The majority of mesh planes constituting the mesh blocks of the computational domain where given symmetry boundary conditions. The numerical code automatically assumes a wall boundary condition for cells intersecting geometric forms as was done for each of the cells encountering the geometries of the corrugations and baffles. Exceptionally, the entrance of the upstream mesh block was defined to have a volumetric flow rate boundary and the exit of the lower mesh block was defined as a pressure boundary with a fixed water level below the ramp. The chosen boundary conditions allow flow to move into the domain, over each of the baffles and exit the computational domain at the downstream end. Flow was initiated from rest throughout the computational domain with fluid regions chosen to be as near as possible to the steady state flow depth (in order to decrease simulation times) for each of the pools.

4.3 Simulations

As a first step, a preliminary model was simulated with baffles having geometries respecting the DFO guidelines for baffle used in culverts. Interested readers may refer to the DFO's technical report for the specific details of the DFO's baffle design [5]. A number of simulations were performed to determine the flow rate which caused the DFO passageway to run at full capacity (i.e. water was just about to flow over the weir portion of the baffle). A flow rate of 0.0615 m^3/s was determined. The velocity and turbulent kinetic energy fields at the passageways as well as the VDP in the pools of both the Hannaford design and the DFO design were compared at this flow rate. The Hannaford design was further tested at a flow

rate of 0.150 m^3/s which was adequate to cause an appreciable amount of flow through the secondary passageway. Two final simulations were performed testing the Hannaford baffle at a slightly higher slope of 10% in order to evaluate the possibility of using the ladder at a steeper gradient. Baffle spacing was adjusted (2.04 m) accordingly to respect the maximum 200 mm drop between the pools.

5. Results and Discussion

5.1 Comparison with DFO baffle - low flow rate

5.1.1 Velocities

As previously stated, excessive velocities are known to impede fish passage at man made and naturally occurring obstacles in streams and rivers. Barrier velocity considerations are of the utmost importance for the design of fish passage structures. Post-processing of the numerical results was performed to obtain the detailed velocity fields in the proximity of the Hannaford and DFO baffle designs. Fig.s 4a and 4b present the near passageway surface velocity magnitude distributions at the 0.0615 m^3/s flow rate. Although the velocity vectors are not shown in figs. 4a and 4b, the flow direction at the passageways can be assumed to be approximately normal to the downstream baffle face. Velocity magnitudes seen in figs. 4a and 4b are within the same order of magnitude, with the highest velocities being roughly 2.5 m/s at the point of entry of the jet at the downstream pool surface. The velocities developed at the passageway for both the Hannaford and DFO baffles are majoritarily below the lower burst swimming threshold for the salmonid species presented in Fig. 1. Juvenile individuals, weaker brown and cutthroat trout as well as non-salmonid species, such as the Artic char may encounter some difficulty at both the Hannaford and the DFO baffle passageways. Further field testing of a full scale Hannaford fish ladder is necessary to verify velocities over a range of common discharges.

5.1.2 Turbulence

Post-processing was also performed to evaluate the turbulent kinetic energy (TKE) distribution near the passageway of both the Hannaford and DFO baffles at the 0.0615 m^3/s flow rate. Figures 4c and 4d depict the near passageway TKE distributions for the Hannaford baffle and the DFO baffle, respectively. Both baffles demonstrate elevated levels of TKE concentrated in the regions where the jet impinges on the corrugations in the downstream pool. The DFO baffles, however, exhibit slightly higher TKE values (>0.05 J/kg) in the proximity of the corrugations compared than that of the Hannaford baffle with values of TKE <0.04 J/kg.

Figures 5 and 6 present streamlines of TKE distribution at the slots and in the pools of a section of the fish ladder. The off-center location of the principal passageway of the Hannaford baffle concentrates the zone of elevated TKE near the side walls of the fish ladder, leaving the center of the pool and the region near the opposing wall with lower values of TKE (<0.020 J/kg). This zone of low TKE may benefit fish passage by providing a large resting zone near the passageway for rest and staging upstream jump attempts. The DFO design demonstrates zones of low TKE to both sides of the jet downstream of the baffle. It can be seen in Fig. 5 that these zones are shallower and smaller, yet still provide resting areas near the upstream passageway with TKE values approximately 0.01 J/kg. The lower TKE magnitudes observed in the Hannaford baffle pools is likely attributed to the increased depth allowing for greater momentum dissipation compared to the shallower DFO design.

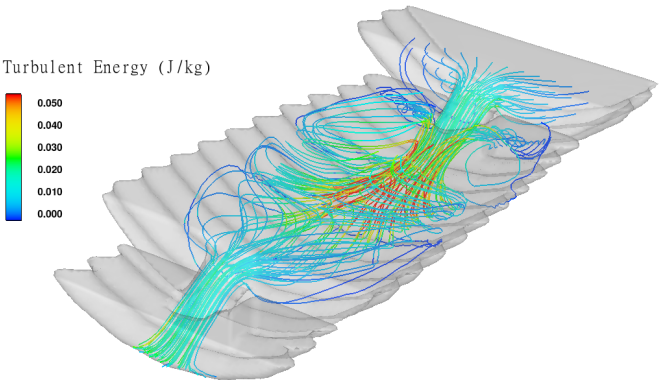

Figure 5. TKE (J/kg) distribution throughout the flow field for the DFO design as depicted along colored streamlines (Q=0.0615 m^3/s).

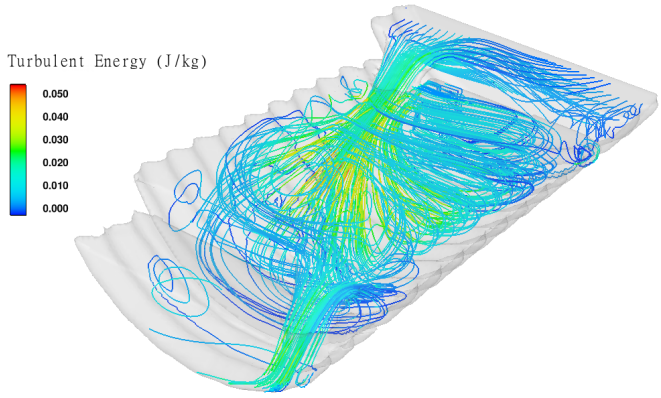

Figure 6. TKE (J/kg) distribution throughout the flow field of the Hannaford baffle as depicted along colored streamlines (Q=0.0615 m^3/s).

The volumetric dissipative power of the Hannaford baffle and the DFO baffles for each of the tested slopes and discharge configurations are presented in Table 1. Both baffle designs respect the VDP suggestions laid out by Larinier et al. 1994 larinier203 for salmonids, with the Hannaford baffle producing roughly half the value of VDP as the DFO baffle. The high hump of the Hannaford baffle helps retain water and build depth in the pools at higher flow rates. This has the advantage of increasing the retained volume in the pool which in turn aids in the reduction of the VDP of the pool.

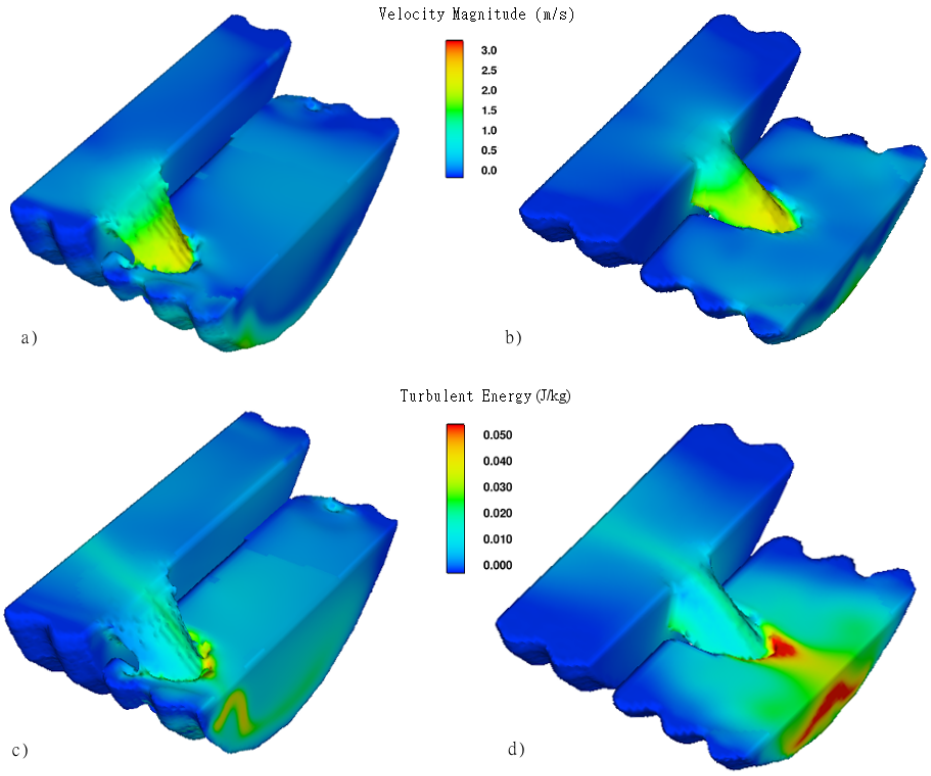

Figure 4. Velocity distribution comparison at the passageways of the (a) Hannaford baffle and the (b) DFO baffle and TKE distributions of the (c) Hannaford baffle and the (d) DFO baffle at the low flow rate of 0.0615 m^3/s.

Consequently, turbulence levels are expected to be lower in the Hannaford fishway which will benefit fish by increasing the volume of refuge areas available in each pool.

Table 1. VDP of the DFO and Hannaford Baffle for at both slopes and discharges.

Baffle Type	Slope	Flow Rate (m^3/s)	VDP (W/m^3)
DFO	8.5%	0.062	125
Hannaford	8.5%	0.062	60
Hannaford	8.5%	0.150	117
Hannaford	10%	0.062	70
Hannaford	10%	0.150	140

5.1.3 Drop heights and Pool Depth

At the low flow rate of 0.0615 m^3/s, the elevation difference between the downstream and upstream water levels for both baffles fluctuates close to 0.2 m. This is well below the maximum jump height of 0.635 m determined by Kondratieff et al. (2006) Kondratieff2006361 for brook trout with body lengths between 10-15 cm. The pool depth near the upstream passageway developed by the Hannaford baffle (approx. 0.495 m) and the DFO design (approx. 0.250 m) also respect the minimum pool depth suggested by Kondratieff et al. (2006) [19] of 10 cm.

5.2 Hannaford Baffle at High flow rate

The surface velocities and TKE distributions at the primary and secondary passageways of the Hannaford baffle at the high flow rate of 0.150 m^3/s are presented in Figs. 7a and 7b. From Fig. 7a it can be seen that the surface velocities at the high flow are in the range of 2 to 2.5 m/s. These values still respect the burst swim speeds of the majority of fish species presented in Fig. 1.

Figure 8 presents the velocity distribution at the baffle and throughout the pool of the Hannaford fish ladder along seeded streamlines in the flow at the high flow rate of Q = 0.150 m^3/s. From Fig. 8, it can be seen that the regions of high velocity ($>$1 m/s) are relegated to the sides of the fish ladder in the wake of the principal and secondary jets. The remainder of the pool is characterized by velocity magnitudes $<$1 m/s.

At the higher flow rate of 0.150 m^3/s the secondary passageway begins to develop enough flow to provide for fish passage. At the principal passageway, the Δh between the upstream and downstream water surface elevations is again approx. 0.2 m. At the secondary passageway the Δh between the downstream water level and the upstream water level is (approx. 0.2 m), whereas the Δh between the downstream wa-

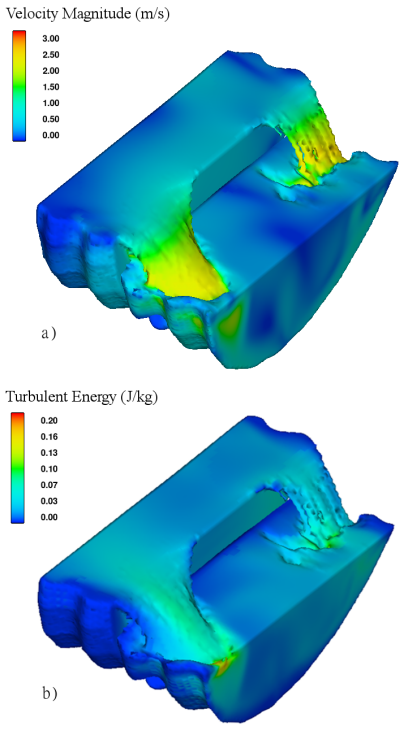

Figure 7. Velocity and turbulent energy distribution through the principal and secondary passageways at the high flow rate (Q = 0.150 m^3/s for the Hannaford baffle.

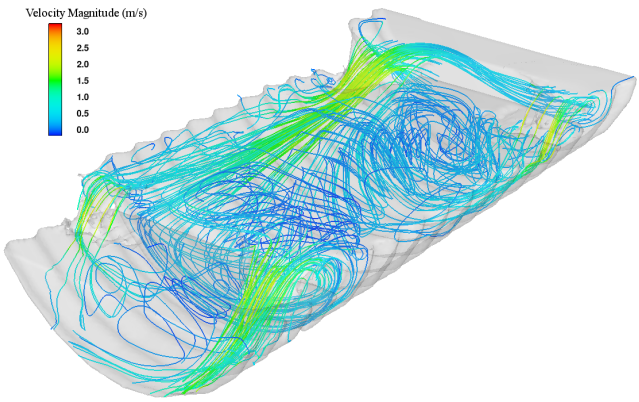

Figure 8. Velocity distribution through the principal and secondary passageways along particle paths at the high flow rate (Q = 0.150 m^3/s).

ter surface elevation and the lowest elevation of the secondary baffle is approx. 0.1 m. These jump heights also fall well below the maximum jump heights demonstrated for brook trout by Kondratieff et al. (2006) Kondratieff2006361.

It is interesting to note however, that the downstream water surface level is higher than the lowest point of the primary passageway by 0.08 m. This can be seen in the profile section of the flow at the principal passageway in Fig. 9b. This has the implication that weaker fish may swim directly between pools without the need to jump. Further increases in flow rate would result in the water surface level of the downstream pool approaching the lower elevation of the secondary passageway.

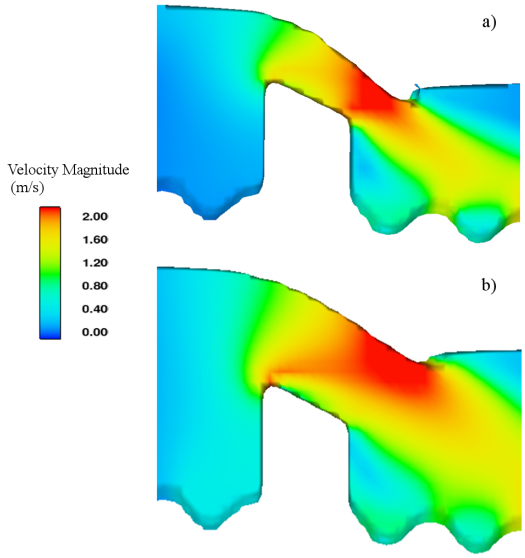

Figure 9. Velocity at the center-line of the principal passageway of the Hannaford baffle at (a) low flow and (b) and the high flow rate (Q = 0.150 m^3/s).

The TKE distribution of the Hannaford baffle at the high flow rate is depicted by particle streamlines in Fig. 10. It is useful to note that the color contour scale of Fig. 10 is not identical to figs. 6 and 5. At the high flow rate the TKE values in the pool increase considerably and range from approx. 0.1 J/kg near the wall downstream of the principal passageway to less than 0.02 J/kg in the more tranquil sections of the pool.

An appreciation of the general flow structure of the pool is important to identify zones of hydraulic refuge and other important hydraulic phenomena that may affect fish passage such as zones with persistent surging upwells and downwells. The flow structure of the entire pool can be visualized from the particle paths in both figs. 8 and 10.

In Fig. 8, the majority of the flow is seen to pass through the principal passageway, dissipating momentum over the side wall corrugations before impinging on the downstream baffle wall from where it is diverted up and then over the proceeding baffle. Flow from the secondary passageway falls along the opposite wall and then is washed towards the center of the pool along the bottom. From here, a horizontal vortex develops

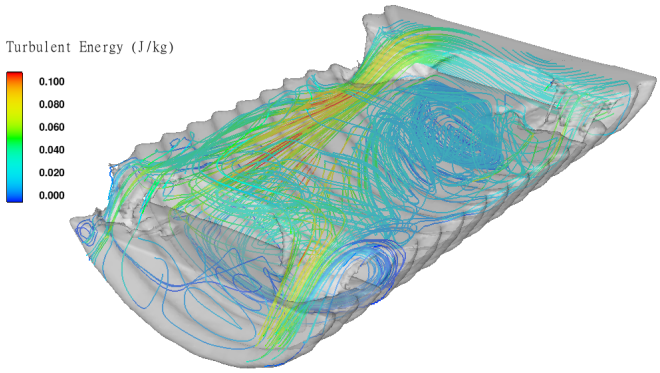

Figure 10. TKE distribution throughout the flow field as depicted along colored particle paths at the high flow rate (Q = 0.150 m^3/s).

into a upwelling vertical vortex near the main downstream passageway.

The fact that the upstream jet dissipates along the wall relegates a significant amount of energy dissipation to a small area of the pool. This design feature reduces the values of TKE in the center of the pool and near the upstream baffle (see Fig. 10). A large volume of water exhibiting low velocity magnitudes and low TKE values is situated close to the upstream baffle between the outfall of the principal and secondary passageways. The location of this zone of hydraulic refuge is ideally suited for fish to rest and stage upstream jump attempts.

Another consideration, fish exiting upstream of the secondary baffle would likely encounter excessive velocities caused by the jet of the main upstream passageway. This may or may not prove inhibitory to fish movement, however in the case that it is, a possible remedy would be the installation of a flow deflector placed approximately 70 cm upstream of the secondary passageway to divert flow up and away from the immediate path of fish exiting upstream of the secondary passageway. Fish could then pass underneath the deflected flow along the bottom of the pool. Further testing is needed to confirm that the addition of such a deflector does not drastically change the hydraulic conditions in the pool.

5.3 Results of the 10% slope

Subsequent simulations were performed on the Hannaford baffle at the slightly higher slope of 10%. Analysis of the simulation results demonstrated similar velocity magnitudes, TKE and general flow structure in the pool as observed for the 8.5% slope (results not shown here). The volumetric dissipative power increased to 140 W/m^3 compared to 110 W/m^3 at 8.5% at the high flow rate (see Table 1), this is due to the reduction in volume caused by the closer baffle spacing necessary on higher slopes to maintain the maximum 0.200 m drop. Placement of the fish ladder on slopes greater than 10% will require very close baffle spacing if a maximum drop height of 0.200 m is to be respected. The maximum possible slope will likely be limited to one producing values of VDP$<$200 W/m^3 as suggested by Larnier et al. (1994) for salmonids. Results from the present study, however, suggest that the Hannaford baffle is well suited to produce adequate hydraulic conditions for fish passage at slopes up to 10%.

6. Recommendations and Practical Considerations

Exhaustive field testing of the Hannaford baffle should be performed to verify the velocity and turbulent flow fields over a range of naturally occurring flow rates. A comprehensive study involving the passage of live specimens would be beneficial to evaluate the design's effectiveness for fish passage. Other considerations, such as the placement of large boulders in the interior of the fish passage and the addition of the flow deflector previously mentioned are possible subjects of future research.

A number of design considerations should also be addressed through a field assessment of a prototype model. The first upstream baffle should be placed in such a manner as to back up the flow in the culvert to ensure an adequate depth for fish passage. Care should be taken to ensure that the hydraulic capacity of the culvert is not severely affected by the addition of the fish ladder (i.e. signifigantly restricting the outlet area). The self-cleaning capability of the Hannaford baffle would also be best studied in the field, yet could be preliminarily investigated with CFD. The invert at the downstream end should be anchored in such a fashion as to align the lowest elevation in the center of the principal passageway with the lowest downstream seasonal water level. The construction of a scour pool would be beneficial to ensure a constantly adequate downstream surface level. Improper installation of the ladder's downstream invert may cause a perched condition with the first downstream baffle acting as a vertical drop during seasonally low flows.

7. Conclusions

The results from this CFD study, while needing field validation, demonstrate that the Hannaford baffle produces similar hydraulic characteristics to that of the Departement of Fisheries and Oceans. The Hannaford baffle produced lower values of VDP and TKE comparable to the DFO design, it also presents the advantage of confining the zones of high TKE and velocity magnitudes near the corrugations allowing a large and relatively tranquil recirculation zone to form just downstream of the upstream baffle, providing access to the passageways. The Δh values of the principal passageway of the Hannaford baffle were found to be below reasonable limits for salmonids species during low flows. At high flows, it was determined that the principal passageway will act as a drowned weir and that fish are likely to be able to swim directly between pools without the need to jump. The secondary passageway was also shown to develop adequate velocities and Δh values for use by fish during higher flow rates. The

flow structure of the pool was analyzed and a large hydraulic refuge zone was identified in close proximity to the upstream baffle which fish may use to rest and stage jump attempts through the passageway. The wide widths of the principal and secondary passageways are thought to improve upstream jumping success rates as suggested by Brant et al. (2005) [18].

The proposed polymer coated corrugated steel fish ladder equiped with the Hannaford baffles, provides a readily installed, lightweight and durable solution to fish habitat fragmentation issues at perched culverts.

Acknowledgments

The authors would like to extend their gratitude to the National Science and Engineering Research Council of Canada as well as the Corrugated Steel Pipe Institute for the financial support needed to pursue this study.

References

[1] J.R. Norman, M.M. Hagler, M.C. Freeman, and B.J. Freeman. Application of a multistate model to estimate culvert effects on movement of small fishes. *Transactions of the American Fisheries Society*, 138(4):826–838, 2009.

[2] J.C. Davis and G.A. Davis. The influence of stream-crossing structures on the distribution of rearing juvenile pacific salmon. *Journal of the North American Benthological Society*, 30(4):1117–1128, 2011.

[3] K. Doehring, R.G. Young, and A.R. McIntosh. Factors affecting juvenile galaxiid fish passage at culverts. *Marine and Freshwater Research*, 62(1):38–45, 2011.

[4] B.C. Harvey and S.F. Railsback. Effects of passage barriers on demographics and stability properties of a virtual trout population. *River Research and Applications*, 28(4):479–489, 2012.

[5] R. Savoie and D. Haché. *Design Criteria for Fish Passage in New or Retrofit Culverts in the Maritime Provinces.* Fisheries and Oceans, 2002.

[6] Charles H. Clay. *Design of Fishways and Other Fish Facilities*. Lewis, 2nd edition, 1995.

[7] C. Katopodis and R. Gervais. Ecohydraulic analysis of fish fatigue data. *River Research and Applications*, 28(4):444–456, 2012.

[8] Milo C. Bell. *Fisheries Handbook of Engineering Requirements and Biological Criteria.* U.S. Army Corps of Engineers, 3rd edition, 1990.

[9] S. J. Peake. Swimming performance and behaviour of fish species endemic to newfoundland and labrador: A literature review for the purpose of establishing design and water velocity criteria for fishways and culverts. Technical Report Canadian Manuscript Report of Fisheries and Aquatic Sciences No. 2843, Fisheries and Oceans Canada, St. John's, NL, February 2008.

[10] D.L. Smith, E.L. Brannon, and M. Odeh. Response of juvenile rainbow trout to turbulence produced by prismatoidal shapes. *Transactions of the American Fisheries Society*, 134(3):741–753, 2005.

[11] A.T. Silva, C. Katopodis, J.M. Santos, M.T. Ferreira, and A.N. Pinheiro. Cyprinid swimming behaviour in response to turbulent flow. *Ecological Engineering*, 44:314–328, 2012.

[12] P. Fouché and R. Heath. Functionality evaluation of the xikundu fishway, luvuvhu river, south africa. *African Journal of Aquatic Science*, 2013.

[13] Nallamuthu Rajaratnam, Gary Van der Vinne, and Christos Katopodis. Hydraulics of vertical slot fishways. *Journal of Hydraulic Engineering*, 112(10):909–927, 1986.

[14] J. Chorda, M.M. Maubourguet, H. Roux, M. Larinier, L. Tarrade, and L. David. Two-dimensional free surface flow numerical model for vertical slot fishways. *Journal of Hydraulic Research*, 48(2):141–151, 2010.

[15] M. Larinier, J.P. Porcher, F. Travade, and C. Gosset. *Passes à poissons - Expertises et conception des ouvrages de franchissement*. Conseil Supérior de la pêche, 1994.

[16] D.V. Lauritzen, F. Hertel, and M.S. Gordon. A kinematic examination of wild sockeye salmon jumping up natural waterfalls. *Journal of Fish Biology*, 67(4):1010–1020, 2005.

[17] M.C. Kondratieff and C.A. Myrick. Two adjustable waterfalls for evaluating fish jumping performance. *Transactions of the American Fisheries Society*, 134(2):503–508, 2005.

[18] M.M. Brandt, J.P. Holloway, C.A. Myrick, and M.C. Kondratieff. Effects of waterfall dimensions and light intensity on age-0 brook trout jumping performance. *Transactions of the American Fisheries Society*, 134(2):496–502, 2005.

[19] M.C. Kondratieff and C.A. Myrick. How high can brook trout jump? a laboratory evaluation of brook trout jumping performance. *Transactions of the American Fisheries Society*, 135(2):361–370, 2006.

[20] D.V. Lauritzen, F.S. Hertel, L.K. Jordan, and M.S. Gordon. Salmon jumping: Behavior, kinematics and optimal conditions, with possible implications for fish passageway design. *Bioinspiration and Biomimetics*, 5(3), 2010.

[21] A.T. Silva, J.M. Santos, M.T. Ferreira, A.N. Pinheiro, and C. Katopodis. Passage efficiency of offset and straight orifices for upstream movements of iberian barbel in a pool-type fishway. *River Research and Applications*, 28(5):529–542, 2012.

[22] W. Rodi. *Turbulence models and their application in hydraulics: a state of the art review.* International Association for Hydraulic Research (IAHR), 1980.